

Accepted for publication in Astrophysical Journal Letters June 30, 2009

Milagro Observations of Multi-TeV Emission from Galactic Sources in the Fermi Bright Source List

A. A. Abdo,^{1,2} B. T. Allen,^{3,4} T. Aune,⁵ D. Berley,⁶ C. Chen,³ G. E. Christopher,⁷ T. DeYoung,⁸ B. L. Dingus,⁹ R. W. Ellsworth,¹⁰ M. M. Gonzalez,¹¹ J. A. Goodman,⁶ E. Hays,¹² C. M. Hoffman,⁹ P. H. Hütemeyer,¹³ B. E. Kolterman,⁷ J. T. Linnemann,¹ J. E. McEnery,¹² T. Morgan,¹⁴ A. I. Mincer,⁷ P. Nemethy,⁷ J. Pretz,⁹ J. M. Ryan,¹⁴ P. M. Saz Parkinson,⁵ A. Shoup,¹⁵ G. Sinnis,⁹ A. J. Smith,⁶ V. Vasileiou,^{6,16} G. P. Walker,^{9,17} D. A. Williams⁵ and G. B. Yodh³

ABSTRACT

We present the result of a search of the Milagro sky map for spatial correlations with sources from a subset of the recent Fermi Bright Source List (BSL). The BSL consists of the 205 most significant sources detected above 100 MeV by the Fermi Large

¹ Department of Physics and Astronomy, Michigan State University, 3245 BioMedical Physical Sciences Building, East Lansing, MI 48824

² Current address: Space Science Division, Naval Research Laboratory, Washington, DC 20375

³ Department of Physics and Astronomy, University of California, Irvine, CA 92697

⁴ Current address: Harvard-Smithsonian Center for Astrophysics, Cambridge, MA 02138

⁵ Santa Cruz Institute for Particle Physics, University of California, 1156 High Street, Santa Cruz, CA 95064

⁶ Department of Physics, University of Maryland, College Park, MD 20742

⁷ Department of Physics, New York University, 4 Washington Place, New York, NY 10003

⁸ Department of Physics, Pennsylvania State University, University Park, PA 16802

⁹ Group P-23, Los Alamos National Laboratory, P.O. Box 1663, Los Alamos, NM 87545

¹⁰ Department of Physics and Astronomy, George Mason University, 4400 University Drive, Fairfax, VA 22030

¹¹ Instituto de Astronomía, Universidad Nacional Autónoma de México, D.F., México, 04510

¹² NASA Goddard Space Flight Center, Greenbelt, MD 20771

¹³ Department of Physics, University of Utah, Salt Lake City, UT 84112

¹⁴ Department of Physics, University of New Hampshire, Morse Hall, Durham, NH 03824

¹⁵ Ohio State University, Lima, OH 45804

¹⁶ CRESST NASA/Goddard Space Flight Center, MD 20771 and University of Maryland, Baltimore County, MD 21250

¹⁷ Current address: National Security Technologies, Las Vegas, NV 89102

Area Telescope. We select sources based on their categorization in the BSL, taking all confirmed or possible Galactic sources in the field of view of Milagro. Of the 34 Fermi sources selected, 14 are observed by Milagro at a significance of 3 standard deviations or more. We conduct this search with a new analysis which employs newly-optimized gamma-hadron separation and utilizes the full 8-year Milagro dataset. Milagro is sensitive to gamma rays with energy from 1 to 100 TeV with a peak sensitivity from 10-50 TeV depending on the source spectrum and declination. These results extend the observation of these sources far above the Fermi energy band. With the new analysis and additional data, multi-TeV emission is definitively observed associated with the Fermi pulsar, J2229.0+6114, in the Boomerang Pulsar Wind Nebula (PWN). Furthermore, an extended region of multi-TeV emission is associated with the Fermi pulsar, J0634.0+1745, the Geminga pulsar.

Subject headings: gamma rays: observations — pulsars: general — supernova remnants

1. Introduction

The Milagro gamma-ray observatory has performed the most sensitive survey of 1 to 100 TeV gamma rays from the Northern Hemisphere sky (Abdo et al. 2007a,b). The Milagro data set is ideal for searching for new classes of gamma-ray sources. The recent release of the Bright Source List (BSL) by the Fermi collaboration (Abdo et al. 2009) presents such an opportunity by looking for coincidences of > 1 TeV emission with these GeV sources. There are 34 sources in the BSL within Milagro’s field of view that are not associated with extragalactic sources. We present a search of the Milagro data for excesses between 1 and 100 TeV coincident with these 34 potential Galactic sources. The analysis presented here differs from previous analyses (Abdo et al. 2007a,b, 2008) by optimizing the event weighting and Gaussian weighting separately in bins of event size (measured with the fraction of channels hit in the instrument). With the improved analysis and an additional year and a half of data, the sensitivity has increased by 15% to 25%, depending on the spectrum of the source.

2. Analysis and Results

We select Fermi-LAT sources in the field of view of Milagro (with $\delta > -5^\circ$) based on their categorization in the BSL. Sources are selected which are confirmed or potential Galactic sources. Sources that are identified as extragalactic are omitted. Sixteen of the selected sources were categorized in the BSL as confirmed pulsars (PSR) and one is a high-mass X-ray binary (HXB). Five sources have a potential association with an SNR, and 12 have no clear association. For each of these 34 sources, we calculate the statistical significance of the Milagro data at the BSL position and estimate the flux or flux limit under the assumption that the emission is from a single point

source.

The flux measurements given in Table 1 are derived with a similar approach to (Abdo et al. 2007b). The flux is measured with an assumed spectrum of $E^{-2.6}$ without a cutoff. The dependence of the calculated flux on the true spectrum is minimized when the flux is quoted at the median energy of the hypothesized spectrum. The median energy depends on Declination and varies between 32 and 46 TeV for δ in the range of 10° and 60° . At a Declination of -5° , the median energy of the hypothesized spectrum is 90 TeV. We quote the flux for all sources above 3σ at a representative value of 35 TeV. It should be noted that the median energy used is for the assumed spectrum and not experimentally measured. In particular, a source may in fact cut off before 35 TeV (the Crab for example) and our analysis would still report a flux at 35 TeV. The energy spectrum of each reported source is the subject of a paper in preparation.

The results of this search are summarized in Table 1. Of the 34 targets, 14 have a significance greater than 3σ . Six of these are associated with sources or candidates from the first Milagro survey of the Galactic plane (Abdo et al. 2007b). The Crab, MGRO 2019+37, MGRO 1908+06, MGRO 2031+41, and Milagro candidates C3 (likely associated with Geminga) and C4 (likely associated with the Boomerang PWN) are all near LAT GeV sources. In the Milagro data set, the 3σ - 5σ observations are fairly marginal because they cannot be convincingly discerned from background when statistical penalties for searching the entire sky are taken into account. However, with LAT points as a trigger for the search, the statistical penalties are reduced. The probability of a single 3σ false-positive in 34 samples of pure background is only $\sim 4.4\%$. The probability of 4 or more excesses at or above 3σ in 34 trials is $\sim 1.5 \times 10^{-7}$. It is very likely that most of our 3σ excesses are due to multi-TeV emission¹. We, therefore, see strong evidence for multi-TeV emission associated with Galactic LAT BSL sources as a class, even if individual sources are not strong enough to definitively distinguish.

There is some contribution to these measurements from the Galactic diffuse emission, but that contribution is small. We can make a conservative estimate by taking the Milagro measurement of the diffuse emission (Abdo et al. 2008) at its highest value, in the inner Galaxy ($30^\circ < l < 65^\circ$, $|b| < 2^\circ$). Using this value, we expect $5.3 \times 10^{-17} \text{ TeV}^{-1}\text{s}^{-1}\text{cm}^{-2}$ in a 1° bin at 35 TeV, which is only about $\sim 15\%$ contamination for the weakest sources in Table 1. The GALPROP conventional model, for comparison, would only constitute $\sim 3\%$ contamination. The contamination is likely lower than suggested by the Milagro measurement because of unresolved sources, such as many of the sources from Table 1. It has even been suggested (Casanova & Dingus 2008) that most of the Milagro diffuse measurement could be due to unresolved sources. Finally, the Fermi points observed at 3σ in the Milagro data occur near local maxima in the Milagro data. In contrast, the

¹ Alternatively, using the False Discover Rate method (Miller et al. 2001; Hopkins et al. 2002) and requiring an estimate of 1% of the members of the selected candidates to be a false discovery, gives the same list of candidates. Changing the contamination fraction criterion from .01 to .001 (or to 0.1), would have included one fewer (or 3 more) sources, respectively.

diffuse emission is expected to vary slowly across the Galaxy.

3. Discussion

From this analysis, it appears quite common for Galactic 100 MeV - 100 GeV sources to have associated multi-TeV emission. This association is notable for pulsars, where 9 of 16 pulsars from the BSL are on our list of likely multi-TeV emitters. The pulsars in the BSL which have less than 3σ significance in Milagro data tend to lie off the Galactic plane. The pulsars off the plane are typically older, having traveled far from their origin after the kick they received from the initial asymmetric supernova (Gunn & Ostriker 1970). Of the SNR sources on the list, we see 3 of 5. Interestingly, we see only 2 of the 12 unidentified sources. These unidentified sources may be extragalactic and not visible with this analysis which was optimized for high-energy emission.

Figure 1 and 2 shows the regions in the Milagro data around the indicated LAT sources. Eight of the 13 sources are associated with previously reported $>TeV$ sources or candidates:

0FGL J0534.6+2201 is the young Crab Pulsar. Its associated pulsar wind nebula (PWN) is a standard reference source in TeV astronomy.

0FGL J0617.4+2234 is associated with SNR IC443, which is interacting with a nearby large molecular cloud. An associated x-ray feature has been interpreted as a PWN (Olbert et al. 2001), implying the existence of a pulsar, but the no pulsed emission has yet been detected. IC443 was first reported above 1 TeV by MAGIC (Albert et al. 2007) and later confirmed by VERITAS (Humensky et al. 2008). The flux reported in Table 1 is somewhat higher than the flux predicted by extrapolating the MAGIC fit, but is roughly consistent after allowing for the extremes of the statistical and systematic errors of the two measurements.

0FGL J0634.0+1745 is the Geminga pulsar. Geminga is a relatively old (342 kyr) but very near (169 pc) pulsar (Manchester et al. 2005; Halpern & Holt 1992). It is the most significant Fermi-LAT source in the northern sky, but emission over 1 TeV has only been reported by Milagro as candidate C3 with too low a significance to be classified as a definitive detection. Milagro observes an emission region that is extended by several degrees as shown in Figure 2. The significance reported in Table 1 has been computed assuming point source emission, but if we instead assume that the source is due to emission from an extended region and convolve a 1° Gaussian with the energy-dependent point spread function, the significance at the location of 0FGL J0634.0+1745 increases to 6.3σ . The local maximum of the Milagro excess is at RA=6h32m28s, Dec=17°22m. Given the high significance, we regard this as a definitive detection of extended emission from Geminga. A spatial Gaussian fit to the data yields a region with a standard deviation of $1.30^\circ \pm 0.20^\circ$. For comparison, the analogous fit for the Crab, which is effectively a point source, has a σ of 0.6° . This suggests that the full width at half maximum of the region of emission in the vicinity of Geminga is $2.6^{+0.7}_{-0.9}^\circ$, after accounting for the point spread function. The large extent (implying an emission region of some 5 to 10 pc extent) is likely due to the nearness of the source and may arise from

a pulsar-driven wind; it is consistent with HESS observation of more distant PWN with an angular size of ~ 10 pc. This may also explain why the source has not yet been observed by Imaging Atmospheric Cherenkov Telescopes (Maier et al. 2008).

0FGL J1907.5+0602 is associated with MGRO J1908+06 (Abdo et al. 2007b). This pulsar was discovered by the LAT and is also coincident with AGILE source 1AGL J1908+0613 (Pittori et al. 2009) and EGRET source GEV J1907+557 (Lamb & Macomb 1997). The multi-TeV emission was first reported by Milagro. HESS both confirmed the Milagro detection and was also able to identify this source as extended by $0.21^{+0.07}_{-0.05}^\circ$ (Djannati-Atai et al. 2007). The peak of the Milagro detection occurs at RA=19h6m44s, Dec=5°50m with a 1 sigma error circle of 0.27° and a local peak significance of 8.1σ . The peak of the Milagro emission is 0.3° from the pulsar, but consistent with the pulsar’s location within the measurement error.

0FGL J1923.0+1411 is associated with SNR G49.2-0.7 (W51) which is in a star-forming region and near molecular clouds. Recently, a $> \text{TeV}$ source, HESS J1923+141 (Feinstein et al. 2009), has been detected which is spatially extended and coincident with the Fermi source.

0FGL J2020.8+3649 is associated with MGRO J2019+37. This is the most significant source in the Milagro data set apart from the Crab. The young central pulsar has a period of 104 ms and an estimated age of 17.2 kyr. This source was also detected by AGILE and EGRET. It was AGILE that first identified the GeV pulsations (Halpern et al. 2008) and that discovery was confirmed with Fermi data. The peak of the flux measured by Milagro is at RA=20h18m43s Dec=36°42m with a 0.09° 1-sigma error circle. The position of the excess is $\sim 0.3^\circ$ from the pulsar.

0FGL J2032.2+4122 is a LAT identified pulsar that is spatially coincident with the HEGRA source J2032+41 (Aharonian et al. 2002), MGRO J2031+41, and the MAGIC source J2032+4130 (Albert et al. 2008). The Milagro source was reported (Abdo et al. 2007b) with an extent of 3° , but it appears that the Milagro extended source may be due to two or more overlapping sources with a potential additional diffuse contribution from the highly emissive Cygnus region. The location of the Milagro peak is RA=20h31m43s and Dec=40°40m with a statistical error of 0.3° .

0FGL J2229.0+6114 is coincident with the radio pulsar J2229+6114 which has been previously associated (Halpern et al. 2001) with the EGRET source 3EG J2227+6122. The period of this pulsar is 52 ms, its distance is 0.8 kpc (Kothes et al. 2001), and the age is estimated to be 10.5 kyr and \dot{E} is 2.2×10^{37} ergs/sec (Manchester et al. 2005; Halpern et al. 2001). Milagro detects a 6.6σ excess at the position of the pulsar and a local maximum of 6.8σ . The peak of the Milagro excess is RA=22h28m17s Dec=60°29m with a statistical position error of 0.36. This source was reported as candidate C4 by Milagro in (Abdo et al. 2007b). With the additional data and improved analysis presented here, this source is elevated to a high-confidence detection. Milagro

also identifies this source as clearly not a point source, with a long extension to the south²

The remaining five objects with greater than 3σ excess in the Milagro data have not been previously detected above 1 TeV energies:

0FGL J0631.8+1034 is the radio pulsar J0631+10 (Zepka et al. 1996). This pulsar has a period of 288 ms and an estimated age of 43.6 kyr, a distance of 6.55 kpc and \dot{E} of 1.7×10^{35} erg/s (Manchester et al. 2005). The VERITAS upper-limit for this region is 1.3% of the Crab (Maier et al. 2008).

0FGL J1844.1-0335 is unassociated with any known source. It is an interesting source because it occurs at a Declination at the edge of Milagro’s sensitivity and, if the Milagro observation is real, it is extremely bright above 1 TeV. It is in the region of the Galactic plane surveyed by HESS (Aharonian et al. 2006) but was not detected. To account for the HESS non-detection, the source would have to be extended or have a very hard spectrum extending to high energy.

0FGL J1900.0+0356 has no known associations.

0FGL J1954.4+2838 is coincident with SNR G65.1+0.6 which has been associated with PSR 1957+2831 (Tian & Leahy 2006).

0FGL J1958.1+2848 is a LAT-discovered pulsar that is associated with the EGRET source 3EG J1958+2909 (Hartman et al. 1999).

0FGL J2021.5+4026 is a LAT-discovered pulsar that is coincident with the gamma-Cygni SNR. This source is located in the Cygnus region that is detected by Milagro as having a broad extended excess.

The relationship between the Fermi and Milagro source fluxes and upper limits for these 34 sources is shown in Figure 3. The BSL values for the integral flux are shown with the Milagro measurements of the differential flux at 35 TeV. The 35 TeV fluxes are roughly correlated with the measurements between 100 MeV and 100 GeV but the correlation is not strong, with a correlation coefficient of the 3σ points in log space of only 0.2. One possible explanation for the pulsar variation is that the pulsed emission is expected to be beamed (and thus viewing-angle dependent) and the unpulsed multi-TeV emission is likely unbeamed (Gaensler & Slane 2006). The spectrum that connects the Milagro flux to the Fermi flux is universally softer than 2.0 and closer to 2.3, depending on the source.

We have found that the population of Fermi sources observed at or above 3σ by Milagro is dominated by pulsars and/or their associated PWN. Of the 4 high-confidence Milagro detections

²Note added in press: The Fermi-LAT collaboration has submitted a paper announcing the discovery of a new pulsar – not included in the BSL – with the current best position of RA=339.561, Dec=59.080 (Fermi-LAT Collaboration 2009). Milagro observes a 4.7σ excess at the location of the pulsar. It may be that the large size of the multi-TeV emission associated with 0FGL J2229.0+6114 is in fact due to these two nearby sources.

associated with pulsars of known periodicity and distance, 3 (namely J0534.6+2201, J0634.0+1745, and J2229.0+6114) have \dot{E}/d^2 above 10^{35} ergs s $^{-1}$ kpc $^{-2}$ where \dot{E} is the spin down luminosity and d is the distance to the pulsar. The distance on the fourth (J2020.8+3649) is uncertain. Using the 3-4 kpc distance implied by x-ray measurements (Van Etten et al. 2008) rather than the 12 kpc measurement implied by the pulsar dispersion measurement, it too has \dot{E}/d^2 above 10^{35} ergs s $^{-1}$ kpc $^{-2}$. A similar association with high \dot{E}/d^2 pulsars is reported by HESS (Carrigan et al. 2007). Since the pulsed emission is beamed and the PWN is not, all high \dot{E}/d^2 are possible candidates for multi-TeV emission. We have searched the ATNF pulsar database (Manchester et al. 2005) for northern-hemisphere pulsars with a high \dot{E}/d^2 , which were not reported in the Fermi BSL. Of the 25 highest \dot{E}/d^2 pulsars, there are 10 in the northern-hemisphere and 5 not identified as GeV sources by Fermi. These 5 are J0205+6449, J0659+1414, J1930+1852, J1913+1011 and J1740+1000. Of these, the largest statistical significance was 3.3 standard deviations (PSR J1930+1852), not significant enough to claim this as new source of multi-TeV gamma rays (though follow-up observations are warranted).

Finally, it is interesting to note that of the sources published in the Milagro survey of the Galactic plane (Abdo et al. 2007b), all 4 sources and two of the 4 source candidates are now strongly associated with pulsars, suggesting that most of the Milagro sources are multi-TeV PWN. We also note the high efficiency with which MeV to GeV pulsars are observed above 1 TeV, and a qualitative picture is emerging where the typical Galactic multi-TeV source is a PWN associated with a MeV to GeV pulsar.

We gratefully acknowledge Scott Delay and Michael Schneider for their dedicated efforts in the construction and maintenance of the Milagro experiment. This work has been supported by the National Science Foundation (under grants PHY-0245234, -0302000, -0400424, -0504201, -0601080, and ATM-0002744), the US Department of Energy (Office of High-Energy Physics and Office of Nuclear Physics), Los Alamos National Laboratory, the University of California, and the Institute of Geophysics and Planetary Physics.

REFERENCES

- Abdo, A. A., et al. 2007a, ApJL, 658, L33
- . 2007b, ApJL, 664, L91
- . 2008, ApJ, 688, 1078
- . 2009, ApJS, submitted (arXiv:0902.1340)
- Aharonian, F., et al. 2002, A&A, 393, L37
- . 2006, ApJ, 636, 777

- Albert, J., et al. 2007, *ApJL*, 664, L87
- . 2008, *ApJ*, 675, L25
- Carrigan, S., et al. 2007, in *Proceedings of the 30th International Cosmic Ray Conference*, Vol. 2, 659–662
- Casanova, S., & Dingus, B. L. 2008, *Astropart. Phys.*, 29, 63
- Djannati-Atai, A., et al. 2007, in *Proc. 30th International Cosmic Ray Conference*, Merida, Vol. 2, 831–834
- Feinstein, F., et al. 2009, in *Proceedings of the Sixth Workshop on Science with the New Generation of High Energy Gamma-Ray Experiments*
- Fermi-LAT Collaboration. 2009, private communication
- Gaensler, B. M., & Slane, P. O. 2006, *ARA&A*, 44, 17
- Gunn, J. E., & Ostriker, J. P. 1970, *ApJ*, 160, 979
- Halpern, J. P., & Holt, S. S. 1992, *Nature*, 357, 222
- Halpern, J. P., et al. 2001, *ApJL*, 552, L125
- . 2008, *ApJL*, 688, L33
- Hartman, R. C., et al. 1999, *ApJS*, 123, 79
- Hopkins, A. M., Miller, C. J., Connolly, A. J., Genovese, C., Nichol, R. C., & Wasserman, L. 2002, *AJ*, 123, 1086
- Humensky, T. B., et al. 2008, in *American Institute of Physics Conference Series*, Vol. 1085, 357–360
- Kothes, R., Uyaniker, B., & Pineault, S. 2001, *ApJ*, 560, 236
- Lamb, R. C., & Macomb, D. J. 1997, *ApJ*, 488, 872
- Maier, G., et al. 2008, in *American Institute of Physics Conference Series*, ed. F. A. Aharonian, W. Hofmann, & F. Rieger, Vol. 1085, 187–190
- Manchester, R. N., Hobbs, G. B., Teoh, A., & Hobbs, M. 2005, *AJ*, 129, 1993
- Miller, C. J., et al. 2001, *AJ*, 122, 3492
- Olbert, C. M., Clearfield, C. R., Williams, N. E., Keohane, J. W., & Frail, D. A. 2001, *ApJL*, 554, L205
- Pittori, C., et al. 2009, *A&A*, submitted (arXiv:0902.2959)

Tian, W. W., & Leahy, D. A. 2006, *A&A*, 455, 1053

Van Etten, A., Romani, R. W., & Ng, C.-Y. 2008, *Astrophysical Journal*, 680, 1417

Zepka, A., Cordes, J. M., Wasserman, I., & Lundgren, S. C. 1996, *ApJ*, 456, 305

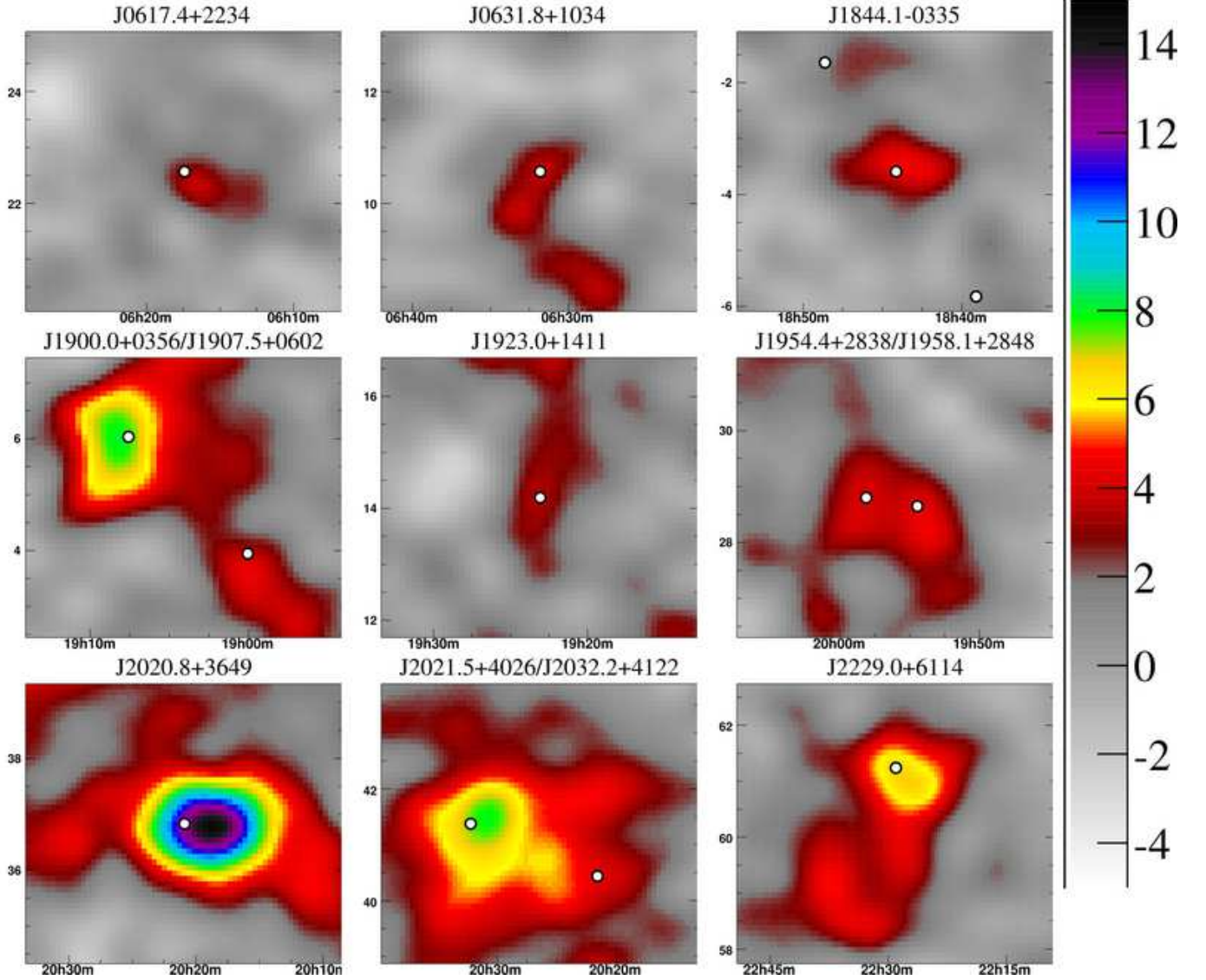


Fig. 1.— The 3σ sources from Table 1, omitting J0634.0+1745 (shown in Figure 2) and the Crab. Each frame shows a $5^\circ \times 5^\circ$ region with the LAT source positions indicated by white dots. The error on the Fermi source locations is quite small on this scale, typically between 0.1 and 0.2 degrees, depending on the source. The data has been smoothed by a Gaussian of width varying between 0.4° and 1.0° , depending on the expected angular resolution of events. Horizontal axes show Right-Ascension and vertical axes show Declination. The colors indicate the statistical significance in standard deviations.

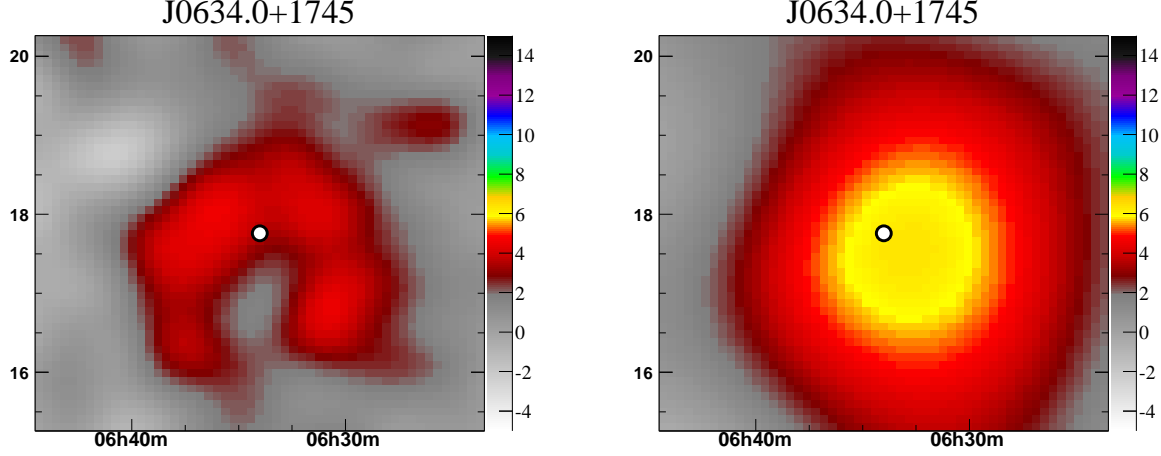


Fig. 2.— The significance of the Milagro data in a $5^\circ \times 5^\circ$ region around Fermi source J0634.0+1745 the Geminga pulsar. The location of the Fermi source is identified by a white dot. The figure on the left shows the significance map after smoothing by the Milagro point-spread function. The figure on the right shows the same region smoothed by an additional 1° Gaussian in order for an extended emission region. The color scale shows the statistical significance.

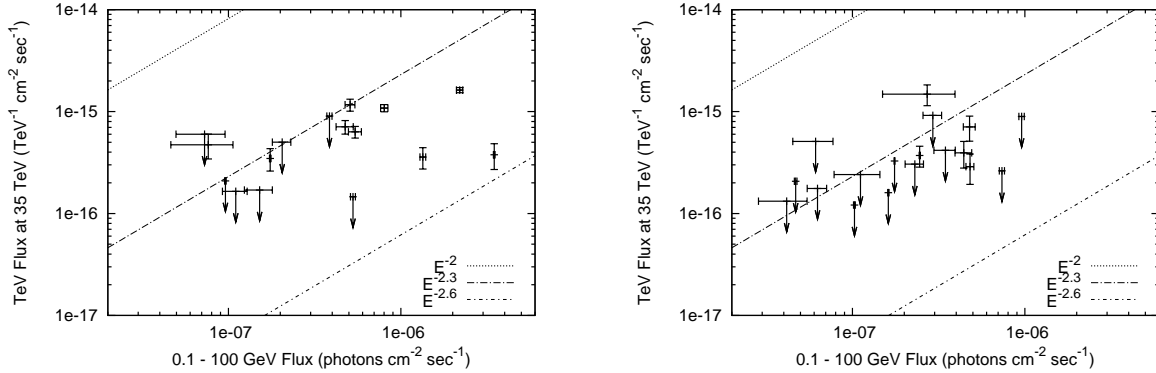


Fig. 3.— Flux estimates and upper limits for the 34 Fermi sources. The horizontal axis quotes the integral Fermi flux from 100 MeV to 100 GeV and the vertical axis gives the Milagro flux or upper limit at 35 TeV. Lines are shown with the extrapolation of the Fermi flux to Milagro energies, assuming an $E^{-2.0}$, $E^{-2.3}$ and $E^{-2.6}$ spectrum. The left panel shows the results for the 16 pulsars and the right panel shows the results for the remaining 18 sources.

Table 1. Summary of the search for TeV emission from sources in the Fermi BSL.

Name (0FGL)	type	RA (deg)	DEC (deg)	l (deg)	b (deg)	Flux ($\times 10^{-17}$ TeV $^{-1}$ sec $^{-1}$ cm $^{-2}$)	Signif. (σ 's)	TeV assoc.
J0007.4+7303	PSR	1.85	73.06	119.69	10.47	< 90.4	2.6	LSI +61 303
J0030.3+0450	PSR	7.60	4.85	113.11	-57.62	< 20.9	-1.7	
J0240.3+6113	HXB	40.09	61.23	135.66	1.07	< 26.2	0.7	
J0357.5+3205	PSR	59.39	32.08	162.71	-16.06	< 16.5	-0.1	
J0534.6+2201	PSR	83.65	22.02	184.56	-5.76	162.6 ± 9.4	17.2	Crab
J0613.9-0202	PSR	93.48	-2.05	210.47	-9.27	< 60.0	-0.0	IC443
J0617.4+2234	SNR ^a	94.36	22.57	189.08	3.07	28.8 ± 9.5	3.0	
J0631.8+1034	PSR	97.95	10.57	201.30	0.51	47.2 ± 12.9	3.7	MGRO C3 Geminga
J0633.5+0634	PSR	98.39	6.58	205.04	-0.96	< 50.2	1.4	
J0634.0+1745	PSR	98.50	17.76	195.16	4.29	37.7 ± 10.7	3.5	
J0643.2+0858		100.82	8.98	204.01	2.29	< 30.5	0.3	
J1653.4-0200		253.35	-2.01	16.55	24.96	< 51.0	-0.5	MGRO J1908+06 HESS J1908+063
J1830.3+0617		277.58	6.29	36.16	7.54	< 32.8	0.2	
J1836.2+5924	PSR	279.06	59.41	88.86	25.00	< 14.6	-0.9	
J1844.1-0335		281.04	-3.59	28.91	-0.02	148.4 ± 34.2	4.3	
J1848.6-0138		282.16	-1.64	31.15	-0.12	< 91.7	1.7	HESS J1923+141
J1855.9+0126	SNR ^a	283.99	1.44	34.72	-0.35	< 89.5	2.2	
J1900.0+0356		285.01	3.95	37.42	-0.11	70.7 ± 19.5	3.6	
J1907.5+0602	PSR	286.89	6.03	40.14	-0.82	116.7 ± 15.8	7.4	
J1911.0+0905	SNR ^a	287.76	9.09	43.25	-0.18	< 41.7	1.5	MGRO J2019+37
J1923.0+1411	SNR ^a	290.77	14.19	49.13	-0.40	39.4 ± 11.5	3.4	
J1953.2+3249	PSR	298.32	32.82	68.75	2.73	< 17.0	0.0	
J1954.4+2838	SNR ^a	298.61	28.65	65.30	0.38	37.1 ± 8.6	4.3	
J1958.1+2848	PSR	299.53	28.80	65.85	-0.23	34.7 ± 8.6	4.0	MGRO J2031+41
J2001.0+4352		300.27	43.87	79.05	7.12	< 12.1	-0.9	
J2020.8+3649	PSR	305.22	36.83	75.18	0.13	108.3 ± 8.7	12.4	
J2021.5+4026	PSR	305.40	40.44	78.23	2.07	35.8 ± 8.5	4.2	
J2027.5+3334		306.88	33.57	73.30	-2.85	< 16.0	-0.2	TEV 2032+41 MGRO J2031+41
J2032.2+4122	PSR	308.06	41.38	80.16	0.98	63.3 ± 8.3	7.6	
J2055.5+2540		313.89	25.67	70.66	-12.47	< 17.6	-0.0	
J2110.8+4608		317.70	46.14	88.26	-1.35	< 24.1	1.1	
J2214.8+3002		333.70	30.05	86.91	-21.66	< 20.7	0.6	MGRO C4
J2229.0+6114	PSR	337.26	61.24	106.64	2.96	70.9 ± 10.8	6.6	
J2302.9+4443		345.75	44.72	103.44	-14.00	< 13.2	-0.6	

Note. — The source identity in the 0FGL catalog is given with the source location in celestial and galactic coordinates. We give the measured flux for all sources above 3σ at a characteristic median energy of 35 TeV. The 2σ upper limits are given for other sources. The statistical significance and nearby TeV associations are noted.

^aThe BSL association with a known SNR is based on similar location.